Proceedings of the 5th World Congress on Momentum, Heat and Mass Transfer (MHMT'20)
~~Lisbon, Portugal~~ Virtual Conference – October 2020
Paper No. ENFHT 227
DOI: 10.11159/enfht20.02

Effects of Supercritical Airfoil Upper Camber Modification on Overall Airfoil Performance

Mushrif Choudhury, Jie Cui, Vahid Motevalli[1]
Tennessee Technological University
1 William L Jones Drive, Cookeville, United States
machoudhur21@students.tntech.edu; JieCui@tntech.edu; vmotevalli@tntech.edu

Abstract **-** This paper explores the effects of a supercritical airplane wing airfoil modification on the aerodynamic characteristics of the wing using primarily lift and drag characteristics. This research is motivated by new approaches in dynamic wing re-configuration studies initiated by NASA. Wing re-configuration via mechanical wing movement has been successfully implemented in military aircraft. The latest approach examines changes in wing characteristics in a dynamic fashion ("morphing") using smart material and moving parts in the entire wing surface. To better understand airfoil modification effects on the aerodynamics of the process, the super-critical airfoil upper camber is varied. ANSYS/Fluent software is used to develop the numerical simulation for compressible flows in the low transonic regime (Mach number 0.7-0.9). The baseline simulations have been successfully validated with published data and selected experimental results. Simulation results for lift, drag, and pressure coefficients along with the flow Mach numbers for various angles of attack have been produced to evaluate airfoil modifications. The preliminary findings point to an improved airfoil lift characteristics by increasing the airfoil upper camber. As expected, increased drag coefficient appear to counteract the improved lift characteristics.

Keywords**:** Airfoil, CFD, Aerodynamic characteristics, Wing morphing

1. Introduction

One of the most promising recent innovations in aircraft design is the development of a morphing wing capable of configuring shape without the use of flaps or other mechanically driven modifications [1]. Determining an optimal airfoil for different flight conditions would be an ultimate goal for a morphing wing. Ideally, such morphing should happen dynamically to provide the best flight performance and aerodynamic characteristics for the wings. The first step in that direction is to understand the aerodynamic characteristics of an airfoil as it is modified. This research examines the effects of altering a key airfoil physical characteristic, i.e. the airfoil upper camber. The aerodynamic analysis is conducted used three-dimensional Computational Fluid Dynamics (CFD) for modified airfoil geometries at different angles of attack.

2. Background

2.1. Literature Review

NASA and MIT collaborated on the development of a composite wing consisting of stiff and flexible components in a base structure "bolted together to form an open, lightweight lattice framework" that is covered in a polymer skin [1]. The resulting structure is controlled by a passive load system that automatically adjusts wing shape to the changes in aerodynamic load conditions detected by sensors installed on the wing, in contrast to actuated control of flaps and slats. These controls are classified as the Mission Adaptive Digital Composite Aerostructure Technologies or MADCAT [1]. As of April 2019, the MADCAT design has been found compatible with a mid-sized plane, successfully completing wind tunnel tests with said plane and "leaving the technology open for future development" [1].

A key component of the aforementioned future development for the MADCAT morphing wing will be the determination of an optimal airfoil for each wing design. Several studies have been conducted on rigid, supercritical wings to determine the effects of physical modification to arrive at an optimal supercritical airfoil. These studies show the direct effects of altering airfoil shape on airplane performance by Hoerner and Borst [2] where the lift coefficients for a composite NACA airfoil were found to increase as the camber-to-chord ratio – i.e. the ratio between the airfoil total camber and the chord length – increased [2]. In addition, a study conducted by Somers [3] concluded that increasing the

[1] Corresponding author

airfoil thickness also leads to an increase in the maximum lift coefficients for NACA airfoils due to roughness regardless of Reynolds number [3].

In order to simulate the supercritical airfoils that could be used by MADCAT, a reference supercritical airfoil with extensive simulations determining lift coefficient and pressure coefficient profiles was identified. The RAE 2822 supercritical airfoil case 9 model was determined to fulfill these criteria [4]. Among the RAE 2822 simulations obtaining lift coefficients include transonic Mach speed recreations by Kumar, et al. [5], a ground effect investigation by Li, et al. [6], and wedge modification studies by Moleyadi [7]. Furthermore, Moelyadi's direct evaluation of lift and drag coefficients versus angles of attack to determine effects of wedge modification made his paper an ideal reference for CFD validation. Moelyadi's utilization of the fourth-order Runge Kutta method in his mesh finite difference analysis ensured mesh grid independence, while the k-epsilon turbulence model he used for calculations ensured that the effects of turbulent flow would accurately portray the flow conditions needed to validate the supercritical airfoil turbulence model used here [7]. The RAE 2822 simulations produced pressure coefficient distributions using unstructured grid turbulence flow simulations by Guillermo Araya [8], boundary layers and wake measurements by Cook et al. [4] and a turbulence model sensitivity assessment and calibration performed by Ronch, et al. [9] in the presence of epistemic uncertainties. Since Cook et al. [4] utilized a wind tunnel to measure and evaluate the pressure coefficient profile of the RAE 2822 airfoil, their pressure coefficient results were used as experimental data validation for the pressure coefficient profile results found here. This wind tunnel was a continuous and closed circuit. Both surface pressure and boundary layer pitot and static pressure tests were conducted in order to calculate the airfoil pressure coefficient profile for the selected wind speed of Mach 0.729 at the 2.79 degree angle of attack [4]. Rahman, et al. [10] obtained RAE 2822 simulations coefficients by numerical simulation including aerodynamic hysteresis at the same Mach number as Cook et al. [4] of 0.729. The computational domain around the RAE 2822 airfoil used by Rahman et al. [10] utilized the 1-equation Spalart-Allmaras turbulent equation model with an identical ANSYS software and domain shape as Araya's [7] template with a drag coefficient range from -4 to 18 degree angles of attack. Therefore, Rahman's [10] paper was an ideal reference for the CFD drag coefficients along with Moelyadi's [7] paper. The prevalence of simulations obtaining both lift coefficients and pressure coefficient distributions made the RAE 2822 an ideal selection for supercritical airfoil performance simulations and allowed an acceptable level of validation for this work.

2.2. Numerical Domain and Boundary Conditions

The RAE 2822 supercritical airfoil baseline simulation was performed using ANSYS Fluent. Guillermo Araya's RAE 2822 turbulence model assessment for the April 2019 MDPI Fluids Journal [8] was used. This simulation utilized the RAE 2822 case 9 model with the following conditions: symmetric wall boundary condition, freestream air flow velocity at Mach 0.729, and compressible air flow at standard temperature and pressure. Finally, the turbulence closure model of Spalart-Allmaras was found to be reliable for the lift and drag simulations [8].

The chord length was set to 1 meter for these simulations. In addition, ensuring that the fully developed air flow could be entirely modeled within the simulation domain compelled inlet and outlet dimensions of at least 10 times the chord length. A hemispherical inlet with radius of 12.5 meters was selected and a rectangular outlet shape with a 12.5 meter width and 25 meter height was selected [5]. The aforementioned model and boundary conditions are enumerated in Table 1.

Table 1: Model and boundary conditions.

Base Airfoil	RAE 2822
Inlet Radius	12.5 meters
Outlet Width x Height	12.5 meters x 25 meters
Chord Length (c)	1 meter
Flow Model	Spalart-Allmaras
Spanwise Boundary	Symmetric
Mach Number	0.729

A 3-dimensional numerical model of the RAE2822 airfoil and its surrounding airflow profile was designed in ANSYS Workbench with a 10 meter span. One face of the numerical model showing the numerical domain is shown in Figure 1a. A magnified view of the airfoil domain focused specifically on the base RAE2822 airfoil itself is shown as Figure 1b. Using Araya's [8] Reynold's number of 6.5 x 10^6, the y+ value for the grid points right above the airfoil surface was chosen to be 1 in order to ensure that all flow details could be captured. Figures 1a-b show the simulation domain. The inlet boundary was split into 400 mesh divisions while the outlet center edge was split into 200 mesh divisions each with a spacing of 0.0625 meters. This resulted in a mesh with 1.3 x 10^6 elements.

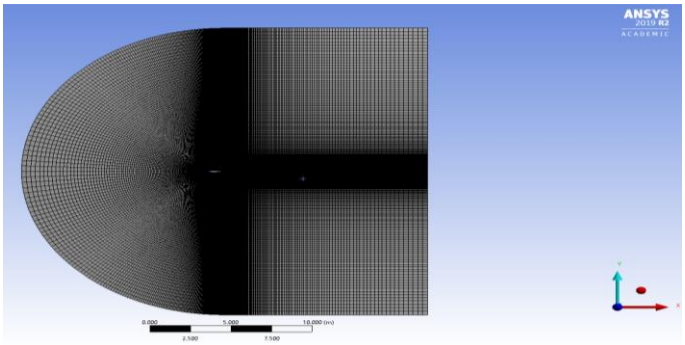

Fig.1a: RAE 2822 numerical domain.

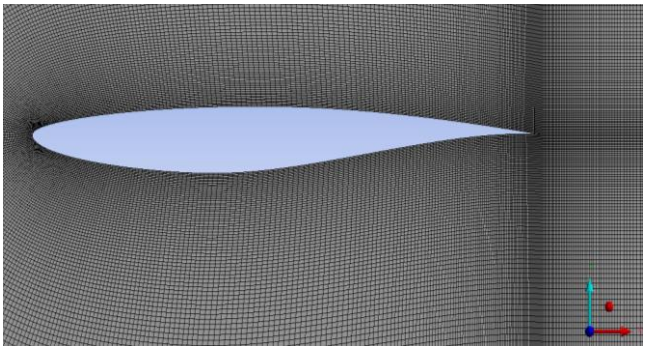
Fig. 1b: RAE2822 magnified numerical domain airfoil view.

3. Results

Preliminary results obtained during the research pointed to the potentially significant effect on the airfoil lift by altering the camber. Since lift is produced by the differences between the upper and lower pressure distribution on an airfoil, we determined that altering the upper camber alone may amplify the effect. In order to determine the effects of upper camber alteration on the RAE 2822 airfoil performance, several levels of increasing and decreasing alterations were used. These levels include the baseline RAE 2822 airfoil and variations of the upper camber in increments of 15% both increasing and decreasing. A geometric representation of the upper camber changes is shown in Figure 2.

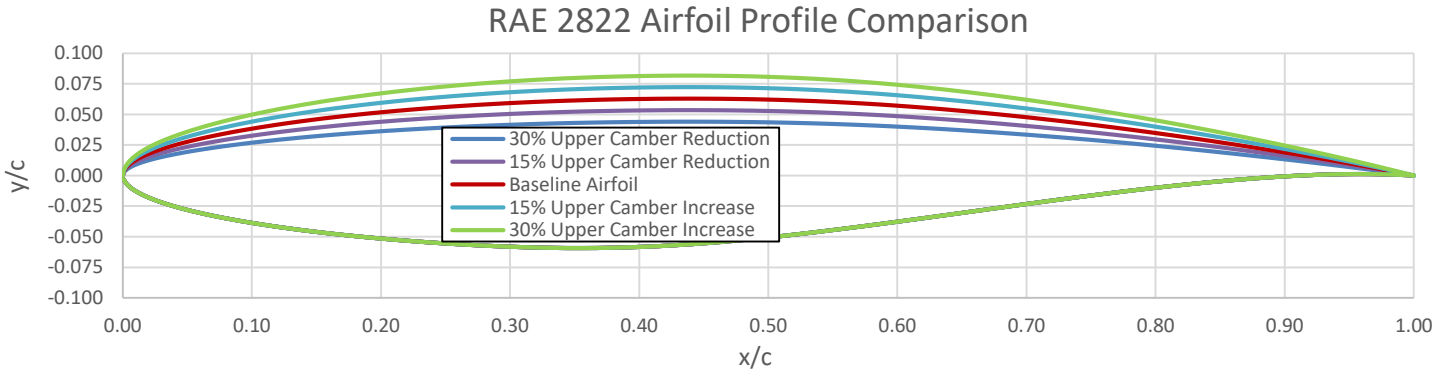

Fig. 2: RAE2822 airfoil profiles with upper camber modification.

The primary airfoil characteristics used to evaluate the airfoil modification effects are lift and drag coefficients further examined by examining pressure coefficient distribution and Mach number variations for the modified airfoil.

3.1. Lift and Drag Coefficients

Lift coefficients were obtained for the angles of attack (AoA) from -4 degrees to 18 degrees. Thus, the stall angle of attack can also be determined. The lift coefficients found for the baseline RAE 2822 airfoil in previous study by Moelyadi

[7] were used to validate the current simulation's lift coefficient profiles. The lift coefficients for both Moelyadi's [7] study and the current simulation are shown in Figure 3.

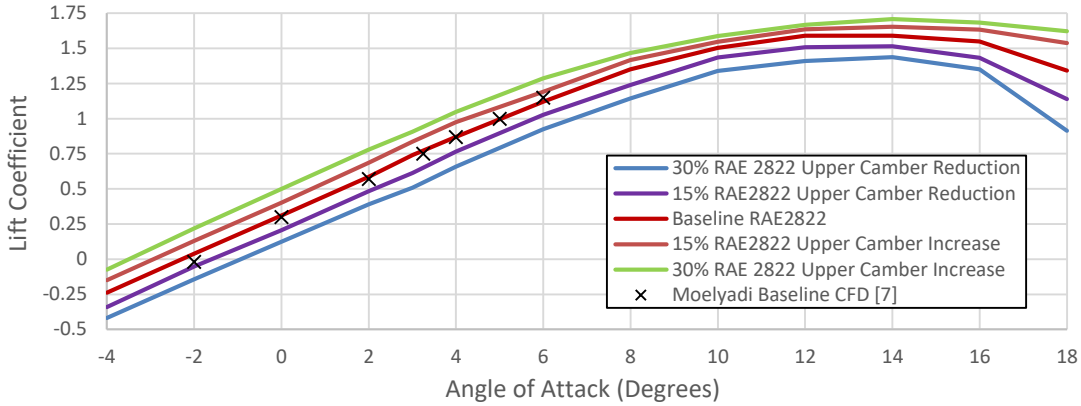

Fig. 3: Lift coefficients for RAE 2822 airfoil at varying AoA and Mach= 0.729.

Figure 3 shows a direct relationship between the upper camber and the resulting lift coefficient for the RAE 2822 supercritical airfoil. As the upper camber increases, the lift coefficient increases. This effect is consistent for the entire range of simulated angles of attack including and beyond the stall angle around 13 degrees. Moelyadi's [7] lift coefficient values for the baseline RAE 2822 airfoil closely validates the current model since they closely match the lift coefficients in the current model at the corresponding angles of attack.

In addition to lift coefficients, drag coefficients were obtained across the same range of AoA. Examining drag coefficients is critical to obtain an overall assessment of the airfoil modification as lift increases can be offset by increased drag. The drag coefficients for the current simulation are shown in Figure 4. These drag coefficient values appear to undergo small but non-negligible changes with the alteration of the upper camber. The drag coefficient result from the simulation appears to be reasonably validated by Moelyadi's [7] and Rahman's [10] baseline RAE2822 CFD data for AoA < 10 degrees. The lift-to-drag ratio is a reasonable first approximation to examine the overall effect of the upper camber modification on the airfoil performance. The lift-to-drag coefficient ratios for all AoAs simulated are shown in Figure 5.

The maximum lift-to-drag coefficient ratio for the RAE 2822 supercritical airfoil is at a 2 degree angle of attack, see Figure 5. The baseline RAE2822 airfoil is shown to have the highest lift-to-drag ratio at this angle of attack. However, an airfoil with 15% increased camber, compared to the baseline case, shows a more consistent lift-to-drag ratio and has a larger range of positive lift. Therefore, while the highest lift-to-drag is achieved by the baseline airfoil, this result clearly shows that a dynamic modification of the upper camber can be used at different AoA to obtain the best possible L/D ratio. The results also indicate that the drag force increase resulting from the upper camber increase may sufficiently counteract the corresponding lift force increase the upper camber. Figure 5 also shows that the L/D remain virtually unaffected by the upper camber modification at AoA > 4 degrees.

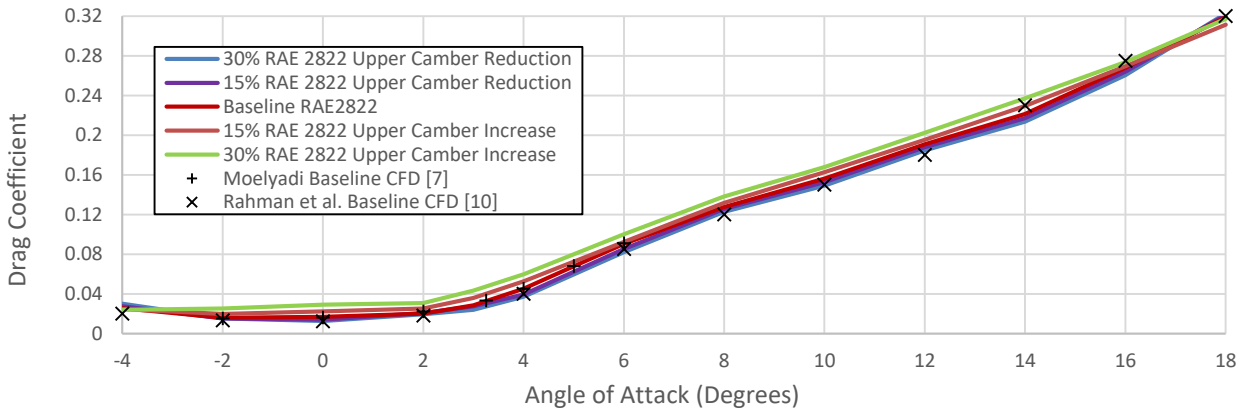

Fig. 4: Drag coefficients for RAE 2822 airfoil at varying AoA and Mach=0.729.

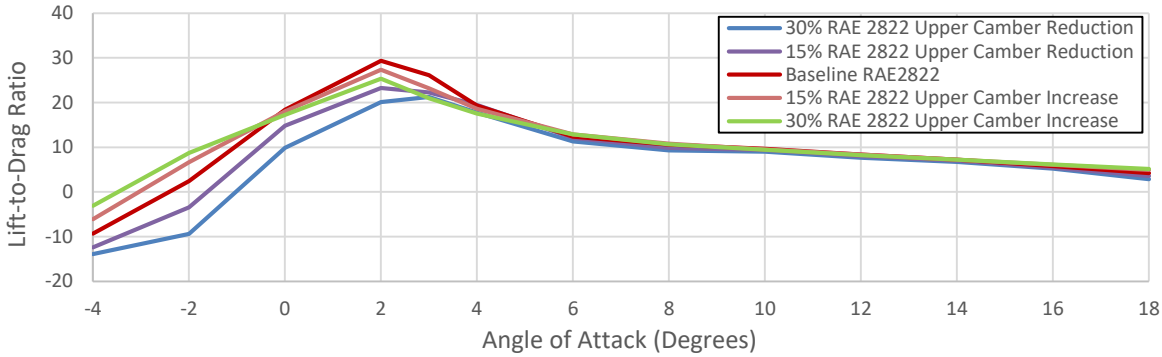

Fig. 5: Lift-to-drag coefficient ratios across RAE 2822 airfoil for varying AoA at Mach 0.729.

3.2. Pressure Coefficient Distribution

Pressure coefficient distributions and contour plots for both the pressure coefficient and Mach number distributions are further examined to better understand the variation of local lift and drag coefficients. These distributions are included here for the AoA of 2.79 degrees, which was used by Cook, et al. [4] to find the pressure coefficient distributions for his RAE 2822 airfoil simulation. The pressure coefficient distributions are shown in Figure 6. The baseline airfoil pressure coefficient distribution in Figure 6 is validated by Cook's [4] baseline airfoil study at the 2.79 degree angle of attack whereby both pressure distributions match very closely. In addition, it can be seen from Figure 7 that as the upper camber increases, the negative pressure coefficient at the upper surface retains a high magnitude for a substantial portion of the airfoil chord length. This results in a higher overall lift when the pressure coefficient difference between the lower and upper airfoil surfaces are calculated and integrated [11]. The baseline airfoil has a high negative pressure coefficient up to approximately 52% of the chord length. Reducing the upper camber reduces the high negative pressure coefficient distribution significantly to 35% of the chord length for a 15% upper camber reduction and to 25% of the chord length for a 30%upper camber reduction. Conversely, increasing the upper camber by 15% increases the extent of the high negative pressure coefficient significantly to 58% percent of the chord length while increasing the upper camber by 30% increases this high negative pressure range to 63% of the chord length. These locations for the range of significant pressure changes will henceforth be referred to as critical chord points. The pressure distribution and the location of these critical chord positions clearly show that increasing the upper camber value of an airfoil increases the overall lift. The lower camber pressure coefficient distributions remain identical for all three airfoil configurations as expected since the lower camber was not changed for any of these new configurations. These simulated pressure coefficient distributions are shown along the RAE 2822 supercritical airfoil as the contour plots in Figures 7a-e.

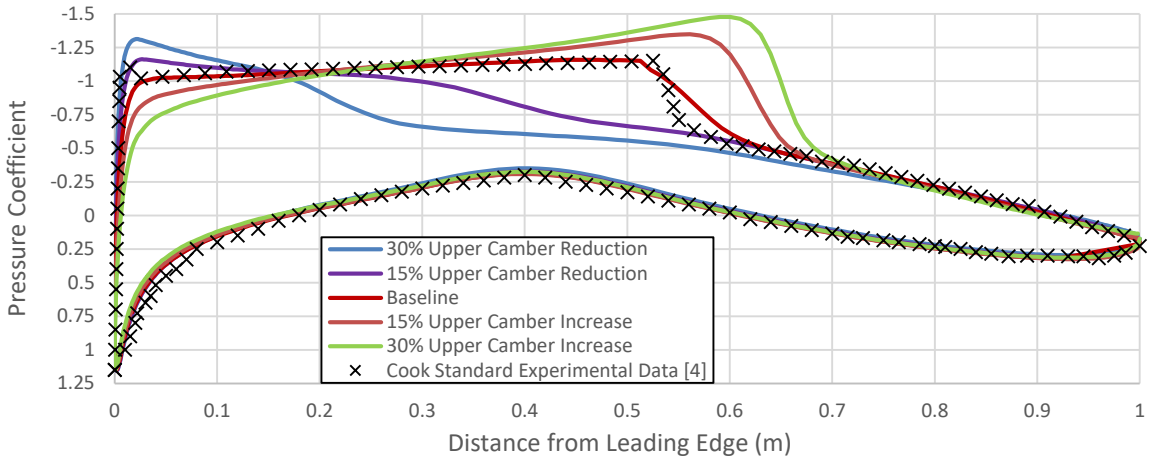

Fig. 6: Pressure coefficient distribution across RAE 2822 airfoil for 2.79 AoA at Mach 0.729.

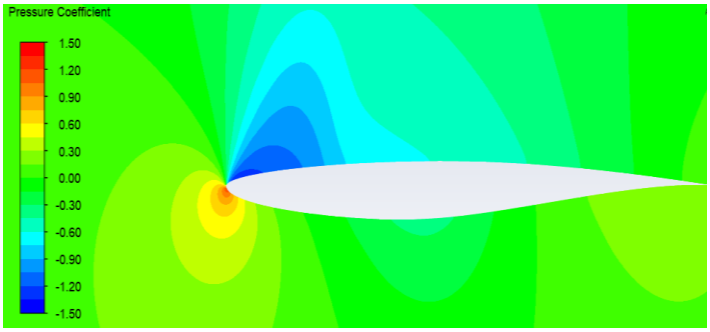

(a) C_p distribution for a 30% upper camber reduction

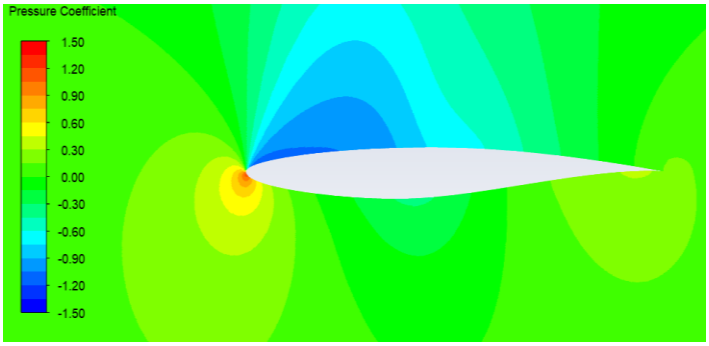

(b) C_p distribution for a 15% upper camber reduction

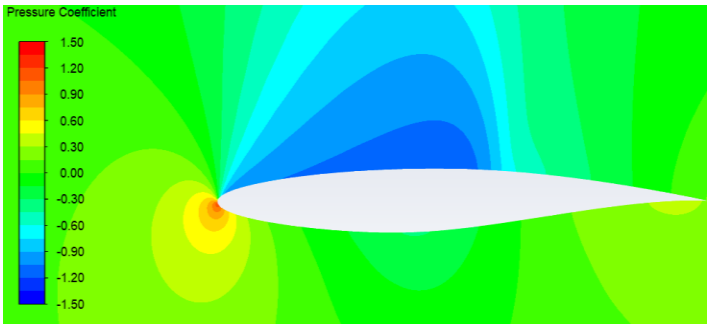

(c) C_p distribution for the baseline

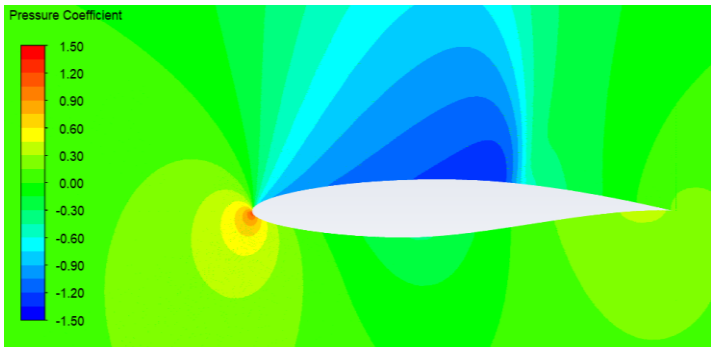

(d) C_p distribution for a 15% upper camber increase

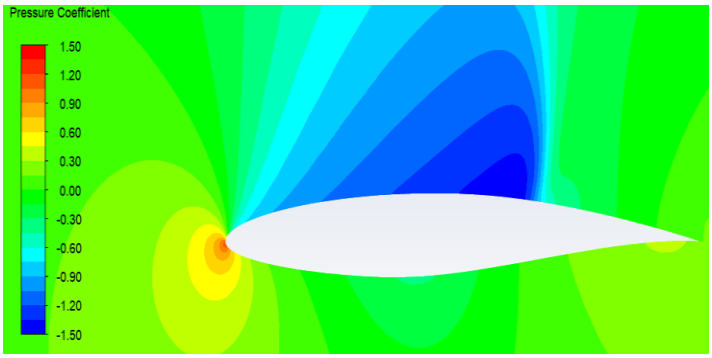

(e) C_p distribution for a 30% upper camber increase

Fig. 7a-e: Pressure coefficient distributions for RAE 2822 airfoil at 2.79 AoA, Mach 0.729.

The largest negative pressure coefficients along the upper airfoil - shown in Figures 7a-e - extends to the critical chord positions consistent with data presented in Figure 5. This further validates the pressure coefficient distributions and impact on the lift distribution shown in Figure 5. Pressure appears to dissipate significantly after reaching this critical chord position, indicating a sudden pressure change. This pressure change indicates the presence of a trailing edge shock wave at the critical chord position. These shock waves induce significant pressure change in the airflow that would result in the sharp pressure spikes shown in Figure 6 at the critical chord positions. These pressure changes appear to converge across a shorter distance as the airfoil upper camber is increased. We can conclude that, as the upper camber thickness increases, the trailing edge shock wave occurs at a larger chord length and the shock wave strengthens as the airfoil upper camber is increased [11].

3.3. Velocity Mach Number Distribution

As indicated in Figure 4, the drag coefficient for the RAE 2822 airfoil increases consistently, but not significantly, as the upper camber is increased. These drag forces are computed by integrating the change in momentum throughout the airfoil. The above discussion of the trailing shock wave location and shock strength directly relates to the changes in the drag force.

The effects of upper camber modification on the flow dynamics and particularly lift and drag forces are further examined by employing the velocity distribution shown as dimensionless Mach number form in Figures 8a-e.

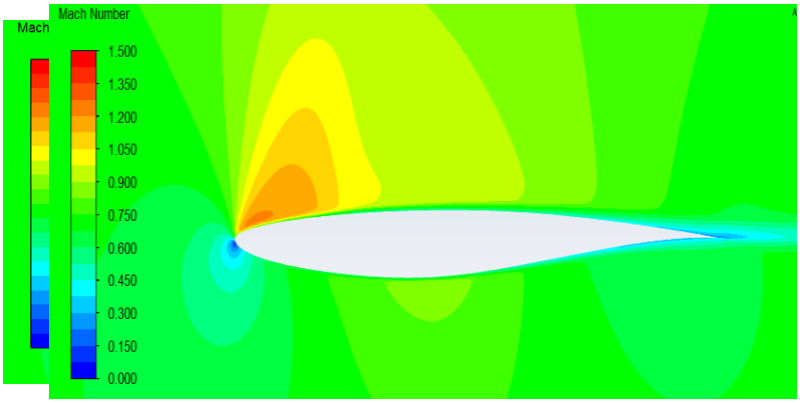

(a) Mach number distribution for a 30% upper camber reduction

(b) Mach number distribution for a 15% upper camber reduction

(c) Mach number distribution for the baseline Mach number

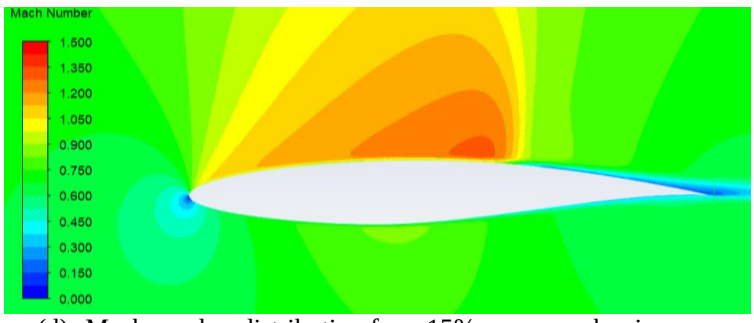

(d) Mach number distribution for a 15% upper camber increase

(e) Mach number distribution for a 30% upper camber increase

Fig. 8a-e: Airflow Mach number profiles along RAE 2822 airfoil for 2.79 AoA.

From Figures 8a-e, the airfoil wake region expands as the upper camber is increased. This wake expansion becomes particularly significant after the upper camber thickness exceeds the baseline airfoil camber size. The expanding wake regions result in increased velocity variation between the upstream flow vs. the trailing edge velocity, thereby increasing the momentum change and resulting drag force along the airfoil [11]. The wake region does not change significantly between the 30% and 15% reduced upper camber configurations from the baseline configuration. The effect of the wake region along with the location of the trailing edge shock wave may be the most significant factors in the changes in the drag coefficient. This is more evident for both the 15% and 30% increased upper camber configurations which correspond to substantially increased drag coefficient for these cases. The evident changes in the airfoil performance based on varying only one physical characteristic of an airfoil indicates that the airfoil performance can be further manipulated by changing other physical characteristics.

3.4 Accuracy and Grid Dependencies

The RAE 2822 ANSYS Fluent simulation model was validated by Moelyadi's [7] and Rahman's [10] data. These comparisons demonstrated the accuracy of the model for the flow conditions of the referenced material. These flow conditions included Mach numbers in the transonic flow range - Mach 0.7 to Mach 1 - where both Moelyadi [7], and Rahman, et. al [10] conducted their simulations for Mach 0.73. The range of angles of attack, where the simulations were validated included the stall angle of attack, approximately 14 degrees, see Figures 3 and 4 and section 3.1. The direct validation of the model from Moelyadi's [7] lift coefficient data from -2 degree to 6 degree angle of attack brings further confidence to the RAE 2822 ANSYS Fluent simulation model within this -2 degree to 6 degree angle of attack range.

In addition to the validation of the simulation with experimental data, a grid-independence evaluation of the CFD model was conducted. Table 2 shows the lift and drag coefficients determined at 2 degree AoA and Mach 0.729 for several numerical grids. Using the same grid distribution, maintaining the total element count of 1.3×10^6 for the RAE 2822 ANSYS simulation results in the variation of lift and drag coefficients within 0.5 percent.

Table 2: Grid independence evaluation of the simulations for the baseline RAE 2822 airfoil (AoA=2°, Mach 0.729

Number of Elements	C_l	C_d
7.5×10^5	0.57434920	0.020675923
1.0×10^6	0.58120466	0.020198225
1.3×10^6	0.58552989	0.019964538
1.5×10^6	0.58553022	0.019964493

4. Conclusion

Increasing the upper camber of a supercritical airfoil is shown to increase the airfoil lift. The lift increase is primarily due to the variation in the pressure distribution, which is induced by the formation of the shock waves and corresponding location of the trailing edge shock wave and its strength. In addition, the airfoil wake region variation can also have a significant effect on the total airfol drag. The lift to drag ratio shows that while the baseline airfoil is clearly optimized to have the best possible L/D at an AoA – which is most likely the design cruising speed AoA – dynamic airfoil modifications at different AoA shows promise and may result in an improved overall performance. The ability to observe airfoil performance variations based on altering only one physical characteristic indicates that further modifications may yield potential improvements as well.

Acknowledgements

The 3-year funding from the College of Engineering at Tennessee Tech for the student author is appreciated.

References

[1] D. Chandler, (2019, March 31). "MIT and NASA Engineers Demonstrate a New Kind of Airplane Wing," MIT News, [Online]. Available: http://news.mit.edu/2019/engineers-demonstrate-lighter-flexible-airplane-wing-0401.

[2] S. Hoerner and H. Borst, *FLUID-DYNAMIC LIFT: Practical Information on AERODYNAMIC and HYDRODYNAMIC LIFT*. 2nd Edition. (1985).

[3] D.M. Somers, "Effects of Airfoil Thickness and Maximum Lift Coefficient on Roughness Sensitivity," National Renewable Energy Laboratory, Subcontractor Report, AAM-7-16479-01, January 2005.

[4] P. Cook, M. McDonald, M. Firmin, "Aerofoil RAE2822 Pressure Distributions and Boundary Layer and Wake Measurements," Report AR-138, AGARD: Paris, France, 1979.

[5] K. Kumar, C. Kumar, and T. Kumar, "CFD Analysis of RAE 2822 Supercritical Airfoil at Transonic Mach Speeds." in *International Journal of Research in Engineering and Technology* vol. 4, Issue 9, pp. 256-262, 2015.

[6] S. Li, D. Zhou , Y. Zhang, and Q. Qu, "Aerodynamic Investigation of RAE2822 Airfoil in Ground Effect." In *Proceedings of the International Conference on Fluid Mechanics, ICFM7*, Qingdao, China, 2015, vol. 126, pp. 174-178.

[7] M. Moelyadi, "Improvement of Transonic Aerofoil Aerodynamic Performance with Trailing Edge Modification Using Wedge Configuration," in *Proceedings of the 23rd International Congress of Aeronautical Sciences* , Toronto, Canada, 2002, pp. 1-9.

[8] G. Araya, "Turbulence Model Assessment in Compressible Flows around Complex Geometries with Unstructured Grids," in *MDPI Fluids Journal*, vol. 4, pp. 1-24, 2019.

[9] A. Ronch, M. Panzeri, J. Drofelnik, and R. D'Ippolitto, "Sensitivity and Calibration of Turbulence Model in the Presence of Epistemic Uncertainties." in *CEAS Aeronautic Journal*, vol. 11, pp. 33-47, 2019.

[10] M. Rahman, A.B.M. Hasan, and M. Labib, Numerical Investigation of Aerodynamic Hysteresis for Transonic Flow over a Supercritical Airfoil," in *Proceedings of BSME International Conference on Thermal Engineering*, Dhaka, Bangladesh, 2014. pp. 368-374.

[11] J. A. Robertson and C.T. Crowe, *Engineering Fluid Mechanics*, 5th edition, Houghton Mifflin, Boston, MA. 1993.